Stabilization of skyrmion textures by uniaxial distortions in noncentrosymmetric cubic helimagnets

A. B. Butenko,[1,2] A. A. Leonov,[1,2,*] U. K. Rößler,[1,†] and A. N. Bogdanov[1]

[1]*IFW Dresden, Postfach 270116, D-01171 Dresden, Germany*
[2]*Donetsk Institute for Physics and Technology, R. Luxemburg 72, 83114 Donetsk, Ukraine*

In cubic noncentrosymmetric ferromagnets, uniaxial distortions suppress the helical states and stabilize skyrmion lattices in a broad range of thermodynamical parameters. Using a phenomenological theory for modulated and localized states in chiral magnets, the equilibrium parameters of the skyrmion and helical states are derived as functions of the applied magnetic field and induced uniaxial anisotropy. These results show that due to a combined effect of induced uniaxial anisotropy and an applied magnetic field, skyrmion lattices can be formed as thermodynamically stable states in large intervals of magnetic field and temperatures in cubic helimagnets, e.g., in intermetallic compounds MnSi, FeGe, (Fe,Co)Si. We argue that this mechanism is responsible for the formation of skyrmion states recently observed in thin layers of $Fe_{0.5}Co_{0.5}Si$ [X. Z. Yu *et al.*, Nature (London) **465**, 901 (2010)].

PACS number(s): 75.30.Kz, 75.10.−b, 75.70.−i

Multidimensional localized and modulated structures (skyrmions) are intensively investigated in many areas of physics.[1,2] In the majority of nonlinear field models, skyrmionic states appear only as dynamic excitations but static configurations are generally unstable and collapse spontaneously into topological singularities.[3] These instabilities can be overcome if the energy functionals contain (i) contributions with higher-order spatial derivatives (*Skyrme mechanism*),[4] or (ii) terms linear with respect to spatial derivatives (so called Lifshitz invariants),[5,6]

$$\Lambda_{ij}^{(k)} = L_i \partial_k L_j - L_j \partial_k L_i, \tag{1}$$

where **L** is a vector order parameter (e.g., the magnetization vector **M** in magnetic materials or the director **n** in chiral liquid crystals), $\partial_k L_i \equiv \partial L_i / \partial x_k$ are spatial derivatives of the order parameter.

In condensed-matter physics, there are no physical interactions underlying energy contributions with higher-order spatial derivatives.[7] On the contrary, the invariants of type (1) arise in systems with intrinsic[8,9] and induced chirality.[6] Particularly, in noncentrosymmetric magnetic materials such interactions stem from the chiral part of spin-orbit couplings (Dzyaloshinskii-Moriya interactions).[8] Chiral interactions of type (1) stabilize helical[8,10] and skyrmionic structures[5,11] with fixed rotation sense (Fig. 1). Theoretically, isolated skyrmions and skyrmion lattices have been investigated for several classes of noncentrosymmetric systems (e.g., see Refs. 2, 6, and 11 and bibliography in Ref. 2). Contrary to uniaxial chiral ferromagnets from Laue classes C_{nv} and D_{2d} where thermodynamically stable skyrmionic states exist in a broad range of applied magnetic fields and temperatures,[2,11,12] skyrmionic states compete with one-dimensionally modulated helices in cubic helimagnets.[2] Hence, in the main part of the magnetic phase diagram for cubic helimagnets, the ordered state helical structures correspond to the global energy minima (such texture have been recently observed in (Fe,Co)Si alloys[13] and in FeGe.[14] Therefore, additional effects are necessary to stabilize skyrmionic

states in these systems.[2,12] In this Brief Report, we demonstrate that uniaxial distortions suppress the helical phases and enable the thermodynamic stability of the skyrmion lattice in a broad range of applied magnetic fields. The calculated magnetic phase diagram allows to formulate practical recommendations on the possibility to stabilize skyrmion states at low temperatures in MnSi, FeGe, (Fe,Co)Si and similar intermetallic compounds with B20 structure.

Following the phenomenological theory developed in Refs. 8 and 10 we write the magnetic energy density for a cubic helimagnet with uniaxial distortions along z axis as

$$w = A(\mathbf{grad\ M})^2 - \mathbf{M} \cdot \mathbf{H} + w_D + w_a - KM_z^2, \tag{2}$$

where A is the exchange stiffness, the second term is the Zeeman energy, $w_D = D(\Lambda_{yx}^{(z)} + \Lambda_{xz}^{(y)} + \Lambda_{zy}^{(x)}) = D\mathbf{M} \cdot \mathrm{rot\ } \mathbf{M}$ is the chiral energy with the Dzyaloshinskii constant D, $w_a = \Sigma_i[B(\partial_i M_i)^2 + K_c M_i^4]$ includes exchange (B) and cubic (K_c) anistropies.[10] The last term in Eq. (2) is uniaxial anisotropy induced by distortions.

The Dzyaloshinskii-Moriya energy w_D [Eq. (2)] favors spatially modulated chiral states where the magnetization rotates with a fixed turning sense in the plane perpendicular to the propagation direction (Fig. 1). The sign and magnitude of the Dzyaloshinskii constant D determine the modulation period and the sense of rotation, respectively. Thus, in zero magnetic field, $\mathbf{H}=0$, and for zero anisotropies, $B=K_c=K=0$, a flat helix forms the magnetic ground state as a *single harmonic* mode with wave number $q_0=D/(2A)$, where the phase angle ϕ of the magnetization varies linearly along the propagation direction ξ, $\phi(\xi)=\xi q_0$.[8,10] Intrinsic cubic anisotropy w_a is much weaker than the energy terms in Eq. (2) and are neglected in further calculations. Its role will be discussed to the end of the Brief Report. The solutions for one-dimensional modulations include (i) distorted helices (*helicoids*) [Fig. 1(a)] and (ii) *conical* phases, helices with the propagation vector along the applied field [Fig. 1(b)].

For the latter state, the equilibrium parameters are readily derived in analytical form
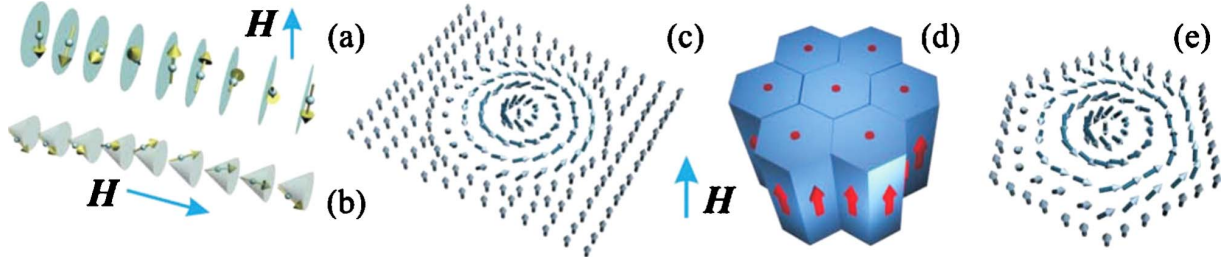
FIG. 1. (Color online) Chiral modulated states in noncentrosymmetric cubic magnets: the *helicoid*, a distorted helix with the propagation direction perpendicular to the applied field (a), the *conical* helix propagates along the applied field (b), an isolated skyrmion (c), a hexagonal skyrmion lattice (d) with the internal structure of the unit cell (e).

$$\cos\theta = \frac{H}{H_0}, \quad \psi = \frac{z}{L_D}, \quad H_0 = H_d\left(1 - \frac{K}{K_0}\right), \quad (3)$$

and the equilibrium energy density $W_C = -K_0 M^2[H^2/(H_0 H_d) - 1]$. In Eq. (3), $L_D = 2A/D$ is the characteristic length unit of the modulated states. In the critical field $H_0(K)$, the conical helix flips into the saturated state. The characteristic field $H_d = D^2 M/(2A)$ is the flip field for zero distortions. The anisotropy value $K_0 = H_d/(2M)$ marks the critical value for uniaxial distortions suppressing the conical phase in zero field. The analytical solutions for helicoids have been derived by Dzyaloshinskii.[8]

In addition to the helical phase, the model Eq. (2) has solutions for two-dimensional modulated states (skyrmions).[5,11] To describe skyrmionic states in a magnetic field along the z axis, we introduce spherical coordinates for the magnetization vector $\mathbf{M} = M(\sin\theta\cos\psi; \sin\theta\sin\psi; \cos\theta)$ and the cylindrical coordinates for the spatial variable $\mathbf{r} = L_D(\rho\cos\varphi; \rho\sin\varphi; z)$. Minimization of energy [Eq. (2)] yields rotationally symmetric solutions $\varphi = \psi + \pi/2$ and $\theta = \theta(\rho)$ derived from equation

$$\frac{1}{\rho}\left(\rho\theta_{\rho\rho} + \theta_\rho - \frac{\sin\theta\cos\theta}{\rho}\right) + \frac{2}{\rho}\sin^2\theta - f(\theta) = 0,$$

$$f(\theta) = (K/K_0)\sin\theta\cos\theta + (H/H_d)\sin\theta \quad (4)$$

with boundary conditions, $\theta(0) = \pi$, $\theta(\infty) = 0$.

Within a circular cell approximation, the equilibrium parameters of skyrmion lattices can be derived by integration of Eq. (4) with boundary conditions $\theta(0) = \pi$, $\theta(R) = 0$ and a subsequent minimization of the lattice energy density $W_{SL} = (2/R^2)\int_0^R w(\rho)\rho d\rho$ with respect to the cell radius R.[5,11] Mathematically similar equations arise for skyrmion states in uniaxial noncentrosymmetric ferromagnets.[11] In particular, there are crystal classes where the Dzyaloshinskii-Moriya energy is described by Lifshitz invariants with gradients only along the directions perpendicular to the unaxial axis, e.g., for D_{2d} classes, $w_D = D(\Lambda_{yz}^{(x)} + \Lambda_{xz}^{(y)})$.[5,15] This restriction of modulations to two dimensions proved to be crucial for the thermodynamical stability of the skyrmion states.[11,12,15] In the high-symmetry cubic helimagnets, the chiral energy $w_D = D\mathbf{M}\cdot\mathrm{rot}\,\mathbf{M}$ [Eq. (2)] energetically favors the helical phases compared to the skyrmion states.[2]

From the numerical investigation of Eq. (4), we now show that a sufficiently strong magnetic anisotropy K stabi-

lizes skyrmionic textures in applied magnetic fields. Typical solutions for $\theta(\rho)$ are plotted in the inset of Fig. 2. At zero field, the skyrmion cells have a smooth distribution of the magnetization [profile (1) in Fig. 2, inset]. An increasing magnetic field gradually squeezes the skyrmion core [profiles (2) and (3)] and transforms the lattice into a system of isolated skyrmions [profiles (4) and (5)]. The skyrmion core size can be introduced in a manner commonly used for magnetic domain walls,[16] $R_0 = \rho_0 + \theta_0/(d\theta/d\rho)_0$, where (ρ_0, θ_0) is the inflection point of profile $\theta(\rho)$ (Fig. 2). The plots in Fig. 2 demonstrate a progressive localization of the skyrmion core R_0 accompanied by the expansion of the lattice cell size R_c with increasing H.

The functional [Eq. (2)] includes two independent control parameters, K/K_0 and H/H_d. The calculated magnetic phase diagram in these variables (Fig. 3) provides a comprehensive analysis of model (2). For $K = 0$, the conical phase is the globally stable state from zero field to the saturation field $(0 < H < H_d)$ (Ref. 10) while metastable solutions for the skyrmion lattices and helicoids exist below the critical fields $H_c/H_d = 0.8132$ and $H_b/H_d = \pi^2/16 = 0.6168$, correspondingly.[2,11] The conical phase is the global minimum of the system within the region (*a*-*A*-*B*-*d*) and trans-
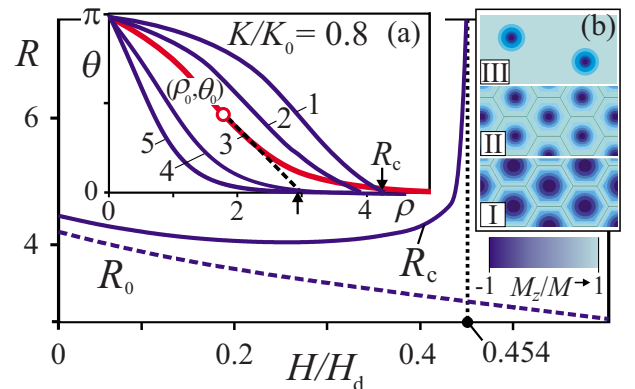

FIG. 2. (Color online) Equilibrium size R_c of the skyrmion cell and the characteristic radius of the core R_0 as functions of an applied magnetic field for $K/K_0 = 0.8$. Inset (a) shows the evolution of skyrmion profiles $\theta(\rho)$ with increasing magnetic field, the distributions of the perpendicular magnetization (M_z) are sketched in inset (b): $H/H_d = 0$ (1, I), 0.2 (2, II), 0.454 (3, III), 0.6 (4), 0.8 (5) profiles (1,2) describe the magnetization in lattice cells (I, II) while profiles (4,5) isolated skyrmions. Profile (3) corresponds to the transition of the skyrmion lattice into a system of isolated skyrmions (III).
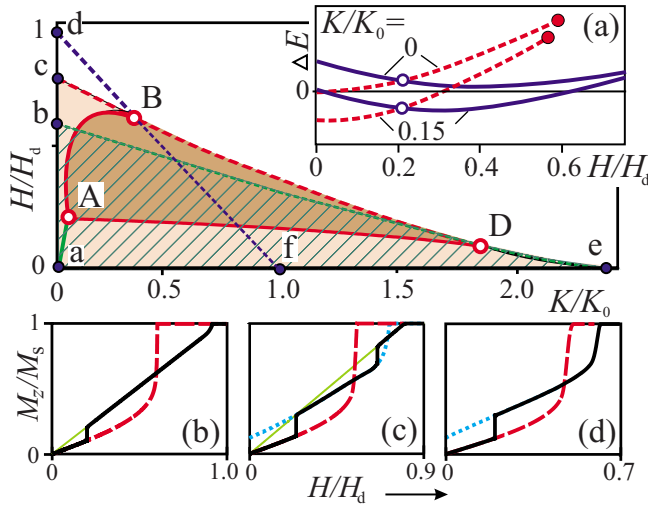
FIG. 3. (Color online) (Color online). Magnetic phase diagram of the solutions for model (2). Filled areas designate the regions of global stability (*A*-*B*-*D*) and metastability (*a*-*b*-*c*-*e*) of skyrmion lattices. These regions transform by first-order processes into the helocoids (*A*-*D*) or conical phases (*A*-*B*). The solutions for helicoids exist within the area (*a*-*b*-*D*-*e*). Inset (a) gives the differences ΔE between the energies for the skyrmion lattice and the conical phase (solid) and the distorted and conical helices (dashed) as functions of the applied field. Insets (b), (c), and (d) show magnetization curves for different values of uniaxial distortions: K/K_0=0.04 (b), 0.4 (c), and 1.6 (d). Solid lines indicate the globally stable phases, metastable states are shown by green thin (conical), red dashed (helicoids), and blue dotted (skyrmions) lines.

forms discontinuously into the skyrmion [(*A*-*B*) line] and helicoid phases [(*a*-*A*) line]. A sufficiently strong *K* suppresses the conical states, and only modulations with the propagation vectors perpendicular to the applied field can exist (helicoids and skyrmion lattices). The skyrmion states are thermodynamically stable within a curvilinear triangle (*A*-*B*-*D*) with vertices (*A*)=(0.050,0.2158), (*B*)=(0.3628,0.6374), and (*D*)=(1.9004,0.10) (Fig. 3). The solutions for helicoids exist within area (*a*-*b*-*D*-*e*). For a certain value of magnetic field the helicoid is transformed into the homogeneous state at the critical line (*b*-*D*-*e*) $D=(\pi/4)\sqrt{AK}[\sqrt{1+\nu}+\text{arcsinh}(1/\sqrt{\nu})]$, where $\nu=H/(2KM)$.[11] Point (*e*) designates the critical value of the anisotropy *K* for the suppression of the modulated states in zero field ($K_e/K_0=\pi^2/4=2.467$).

The critical points *A*, *B*, and *D* separate the phase diagram (Fig. 3) into four distinct regions. (I) In the low anisotropy region ($K<K_A=0.05K_0$) only helical states are realized as thermodynamically stable phases. (II) For $K_A<K<K_B=0.363K_0$, the skyrmion lattice becomes absolutely stable in a certain range of the applied field. The Skyrmionic phase is separated from the helicoidal and conical states by first-order transitions. [inset (c)]. (III) For $K_B<K<K_D=1.90K_0$, the magnetization curve includes a first-order transition between the helicoid and the Skyrmion lattice and the second-order transition of the Skyrmion phase into the saturated state [inset (d)]. (IV) Finally for ($K_D<K<K_e$) the helicoids are thermodynamically stable in the whole region where the modulated states exist.

The equilibrium energies of the conical (W_C), helicoidal (W_H), and skyrmion (W_{SL}) phases plotted as functions $\Delta E_{SL(H)}=W_{SL(H)}-W_C$ versus the applied field [inset (a) of Fig. 3] help to elucidate the physical mechanisms that lead to the formation of the different modulated states. The conical phase has a simple structure with its single-harmonic rotation of the magnetization component $M_\perp=M\sin\theta$ [Eq. (3)]. For zero *K*, i.e., for an isotropic helimagnet this provides a larger reduction in the energy density in an external field ($w_D\propto -DM_\perp^2$) than is possible for the (*anharmonic*) modulations in the alternative phases of helicoids and skyrmion lattices. An increasing uniaxial anisotropy $K>0$ gradually decreases $M_\perp$ [Eq. (3)] and the chiral energy contribution in the energy of the conical phase. Correspondingly, the conical phase becomes unstable with respect to the competing modulated states (Fig. 3).

The energetic advantage of skyrmion states is due to rotation of the magnetization in two dimensions. This (*double twist*) grants a larger reduction in the Dzyaloshinskii-Moriya energy than a single-direction rotation in helical phases. Thus, the double twist yields a lower energy density in the skyrmion cores compared to helical states. On the other hand, the incompatibility of spin configurations near the edges of the hexagonal cells leads to an excess of the energy density in this region.[2] The analysis shows that at zero field this energy cost outweighs the energy gain in the skyrmion core. An increasing external magnetic field antiparallel to the magnetization in the skyrmion center gradually decreases the total energy by suppressing the energy cost near the wall-like structure surrounding the skyrmion cores with the shape of a honeycomb (Fig. 2, inset). At a finite field as marked by the *A*-*D* line in Fig. 3, the skyrmion lattice has lower energy than the alternative helical states. Because the topology of the helix and the skyrmion lattices are different, this field-driven transition has to take place by a first-order process. Thus, *in uniaxially distorted cubic helimagnets the thermodynamical stability of skyrmion lattices is reached as a combined effect of applied magnetic field, that causes the localization of the cell core, and the uniaxial anisotropy to suppress the alternative conical states.*

Skyrmionic states now have been observed in nanolayers of $Fe_{0.5}Co_{0.5}Si$.[17] To explain the stability of the skyrmion phase in this system, we argue that surface-induced uniaxial anisotropy in this system suppresses the cone phase and stabilizes skyrmion and helicoid modulations in crystal plates that are thin enough. The magnetic transformation under field reported for the $Fe_{0.5}Co_{0.5}Si$ films show a first-order process from helicoids at low field into the dense skyrmion phase. At high fields, isolated skyrmions are set free and form disordered ensembles. This sequence of magnetization processes corresponds to the calculated behavior for systems with intermediate uniaxial anisotropy, Fig. 3(d). As seen in Ref. 17, there is a type of melting of the ordered skyrmion lattice at higher fields and temperatures where the free skyrmions form weakly coupled disordered aggregates. These observations correspond to the existence region of free skyrmions in the magnetic phase diagram above the stability range for dense stable skyrmion lattices, which is a feature of the generic phase diagrams for skyrmion phases calculated in Ref. 12. Thus, the experimental observations reported in Ref.

[17], are in close agreement with theoretical predictions on the behavior of skyrmionic phases, as composed of particlelike radial objects (in two spatial dimensions), that remain intrinsically stable beyond the existence range of latticelike condensed phases.[2,11,12]

For MnSi, earlier experiments[18] and analysis[19] of magnetoelastic couplings allow a quantitative estimate showing that the effects predicted here can be achieved in experiment. The magnetoelastic coupling with uniaxial strains u_{zz} is given by $w_{me}=bu_{zz}(M_z/M_S)^2$, where $M_S=50.9$ A/m is the saturation magnetization[20] and $b=7.4$ GPa is a magnetoelastic coefficient derived from the magnetostriction data in Ref. [18]. Using exchange constant $A=0.11$ pJ/m, as estimated from the spin-wave stiffness reported in Ref. [21], and $D=2q_0A$ $=0.86$ μJ/m^2 for MnSi[2] we have $K_0 \simeq 17$ kJ/m^3 and a dimensionless scale $b/K_0 \simeq 44$ for the induced anisotropy. Thus, a modest strain $u_{zz}=0.0024$ is sufficient to reach an induced anisotropy $K/K_0=0.1$ well within the region for stable skyrmion lattices in the phase diagram Fig. 3. This strain corresponds to a tensile stress $\sigma_{zz}=680$ MPa for MnSi by using the elastic constant $c_{11}=283$ GPa.[22] The rather low uniaxial stress necessary to stabilize the skyrmion lattice is particularly relevant for pressure experiments with a uniaxial misbalance of the applied stresses but it could also be achieved in epitaxial films.

Finally, intrinsic anisotropy w_a [Eq. (2)] also makes a contribution to stabilize skyrmionic states as both exchange (B) and cubic (K_c) anisotropies violate the ideal spin configuration of the cone [Eq. (3)] and *increases* the energy of this phase.[12] This favors skyrmion lattices for certain directions of the applied field. Particularly, in MnSi ($B<0$) for skyrmion lattices oriented along [001] type axes $\Delta E_{SL}(H/H_d)$ $=0$ at critical point ($B_{cr}=0.10A/D^2$, $H_{cr}=0.408H_d$). Thus, for $|B|>B_{cr}$ skyrmion lattices are globally stable in a certain interval of magnetic fields around H_{cr}.

In conclusion, we have shown that in cubic helimagnets uniaxial distortions effectively suppress helical states and stabilize the skyrmion states in a broad range of the applied fields.

---

*Corresponding author. FAX: +49-351-4659-490; a.leonov@ifw-dresden.de

†u.roessler@ifw-dresden.de

[1] A. Schmeller, J. P. Eisenstein, L. N. Pfeiffer, and K. W. West, Phys. Rev. Lett. **75**, 4290 (1995); C. Bäuerle, Yu. M. Bunkov, S. N. Fisher, H. Godfrin, and G. R. Pickett, Nature (London) **382**, 332 (1996).

[2] U. K. Rößler, A. N. Bogdanov, and C. Pfleiderer, Nature (London) **442**, 797 (2006); A. N. Bogdanov, U. K. Rössler, and C. Pfleiderer, Physica B **359-361**, 1162 (2005).

[3] G. H. Derrick, J. Math. Phys. **5**, 1252 (1964).

[4] T. H. R. Skyrme, Proc. R. Soc. London **260**, 127 (1961).

[5] A. N. Bogdanov and D. A. Yablonsky, Zh. Eksp. Teor. Fiz. **95**, 178 (1989) [Sov. Phys. JETP **68**, 101 (1989)]; A. Bogdanov, JETP Lett. **62**, 247 (1995).

[6] A. N. Bogdanov and U. K. Rößler, Phys. Rev. Lett. **87**, 037203 (2001).

[7] Energy terms of the fourth order in gradients of the magnetization arise as a continuum limit of discretized models with competing exchange interactions (Ref. 16). These systems are characterized by short modulation periods with spontaneously broken chiral symmetry.

[8] I. E. Dzyaloshinskii, Sov. Phys. JETP **19**, 960 (1964).

[9] P. G. de Gennes and J. Prost, *The Physics of Liquid Crystals* (Clarendon, Oxford, 1993).

[10] P. Bak and M. H. Jensen, J. Phys. C **13**, L881 (1980); O. Nakanishi, A. Yanase, A. Hasegawa, and M. Kataoka, Solid State Commun. **35**, 995 (1980).

[11] A. Bogdanov and A. Hubert, J. Magn. Magn. Mater. **138**, 255 (1994); **195**, 182 (1999).

[12] A. A. Leonov, A. N. Bogdanov, and U. K. Rössler, arXiv:1001.1292 (unpublished).

[13] M. Uchida, Y. Onose, Y. Matsui, and Y. Tokura, Science **311**, 359 (2006).

[14] M. Uchida, N. Nagaosa, J. P. He, Y. Kaneko, S. Iguchi, Y. Matsui, and Y. Tokura, Phys. Rev. B **77**, 184402 (2008).

[15] A. N. Bogdanov, U. K. Rößler, M. Wolf, and K.-H. Müller, Phys. Rev. B **66**, 214410 (2002).

[16] A. Hubert, *Theorie der Domänenwände in geordneten Medien* (Springer, Berlin, 1974); see also P. I. Melnichuk, A. N. Bogdanov, U. K. Rößler, and K.-M. Müller, J. Magn. Magn. Mater. **248**, 142 (2002).

[17] X. Z. Yu, Y. Onose, N. Kanazawa, J. H. Park, J. H. Han, Y. Matsui, N. Nagaosa, and Y. Tokura, Nature (London) **465**, 901 (2010).

[18] E. Franus-Muir, M. L. Plumer, and E. Fawcett, J. Phys. C **17**, 1107 (1984).

[19] M. L. Plumer and M. B. Walker, J. Phys. C **15**, 7181 (1982).

[20] D. Bloch, J. Voiron, V. Jaccarino, and J. H. Wernick, Phys. Lett. A **51**, 259 (1975).

[21] S. V. Grigoriev, S. V. Maleyev, A. I. Okorokov, Y. O. Chetverikov, R. Georgii, P. Böni, D. Lamago, H. Eckerlebe, and K. Pranzas, Phys. Rev. B **72**, 134420 (2005).

[22] S. M. Stishov, A. E. Petrova, S. Khasanov, G. K. Panova, A. A. Shikov, J. C. Lashley, D. Wu, and T. A. Lograsso, J. Phys.: Condens. Matter **20**, 235222 (2008).